Collective lattice excitations in the dynamic route for melting hydrodynamic two-dimensional crystals

Mikheil Kharbedia,[1] Niccolò Caselli,[1,2] Macarena Calero,[1,2,3] Lara H. Moleiro,[1,2] Jesús F. Castillo,[1,2] José A. Santiago,[4,*] Diego Herráez-Aguilar,[5,†] and Francisco Monroy[1,2,‡]

[1]*Department of Physical Chemistry, Universidad Complutense de Madrid , Ciudad Universitaria s/n E28040 Madrid, Spain*
[2]*Translational Biophysics, Instituto de Investigación Sanitaria Hospital Doce de Octubre, Avenida Andalucía s/n, E28041 Madrid, Spain*
[3]*Facultad HM de Ciencias de la Salud, Universidad Camilo José Cela, Villanueva de la Cañada, 28692 Madrid, Spain and Instituto de Investigación Sanitaria HM Hospitales, Madrid, Spain*
[4]*Departamento de Matemáticas Aplicadas y Sistemas, Universidad Autónoma Metropolitana Cuajimalpa, Vasco de Quiroga 4871, 05348 Ciudad de México, Mexico*
[5]*Instituto de Investigaciones Biosanitarias, Universidad Francisco de Vitoria, Carretera Pozuelo-Majadahonda, E28223 Pozuelo de Alarcón, Spain*

(Received 4 April 2024; accepted 9 October 2024; published 14 November 2024)

Liquid surface stiffness generates stable Faraday wave (FW) patterns, known as hydrodynamic crystals, which form resonant FW lattices composed of discrete harmonics and subharmonics under monochromatic driving. Key interactions include inertia-driven parametric resonance, which halves subharmonic modes, and surface rigidity harnessing three-wave coupling, which focuses the nonlinear harmonic wave field. Here, we reveal these wave interaction processes allowing coherent FW packets to organize in space and time while also exciting decoherent disorder in the hydrodynamic crystal lattice. Collective excitations are shown to emerge as dispersionless dislocation waves, causing periodic amplitude modulations due to explicit symmetry breaking. From a field theory perspective, we show chaotic FW degeneration leading to hydrodynamic crystal melting via continuous mode halving under forcing, akin to Landau's theory of chaotic turbulence.

DOI: 10.1103/PhysRevResearch.6.043142

I. INTRODUCTION

Hydrodynamic crystals (HCs)—a paradox of order built in disorder upon broken symmetries [1,2]—represent an exotic state of oscillatory fluid matter emerging from interactions far from equilibrium [3]. Yet fluid, hydrodynamic oscillations can exhibit solidlike properties, such as in microfluidic crystals [4,5]. Hypothetically, intrinsic stiffness would impart hydrodynamic order into waving patterns emerging from losing fluid symmetries [6–8]. In tensioned fluid surfaces, when the liquid is forced against bulk inertia, for instance, the Faraday wave (FW) instability engenders resonant wave fields [9]. Subharmonic FW fields emerge from frequency halving, as a parametric resonance with the driving source [10]. In a previous work, we created freestanding HCs by exciting monochromatic FWs on a rigidized water surface stabilized by a shear-stiffening surfactant [11]. Highly discretized FWs composed of nonlinear capillary waves (CWs)—hereinafter, Faraday-capillary waves (FCWs)—emerge from three-wave interactions [12–14], an exact (conservative) class of resonant coupling [10]. Under sufficient surface-intrinsic rigidity, coherent FCWs appeared self-focused into localized density packets, forming a "frozen" HC lattice with a locked wave phase (see Ref. [11] and Supplemental Material therein). Such freezing of FCW-HC is solely due to surface-intrinsic rigidity, without any bulk stress needed [11], neither elastic [14,15] nor merely frictional [16,17], nor due to extrinsic constraints [18,19].

Nevertheless, the Faraday instability may become the Achilles heel for excited HCs; if newer subharmonic trajectories bifurcate from the "frozen" FCWs [20,21], more subharmonic modes could become "molten" into multiple degenerated states associated with lattice defects [11,22]. Indeed, mode-halving (subharmonic) disorder can lead to slower cascades of disarranging modes growing from localized defects up to larger scales, causing the lattice interactions to disentangle, eventually leading to hydrodynamic crystal melting [23–25]. Previous studies on FW patterns of CWs harnessed by bulk friction treated lattice-disordering modes [15–17] as wave modulations under viscoelastic drag [26,27]. Some authors invoked effective elasticity as a putative regulator, though no material substrate existed for surface wave ordering beyond extrinsic friction [15]. Recently, a quasiperiodic transition from square patterns to defect-riddled states was reported in friction-supported FCW patterns [28]. A lattice-extrinsic, boundary-mediated defocusing mechanism was identified as amplified disorder in the pathway to melting [28].

*Contact author: jasantiagog@gmail.com
†Contact author: diego.herraez@ufv.es
‡Contact author: monroy@ucm.es

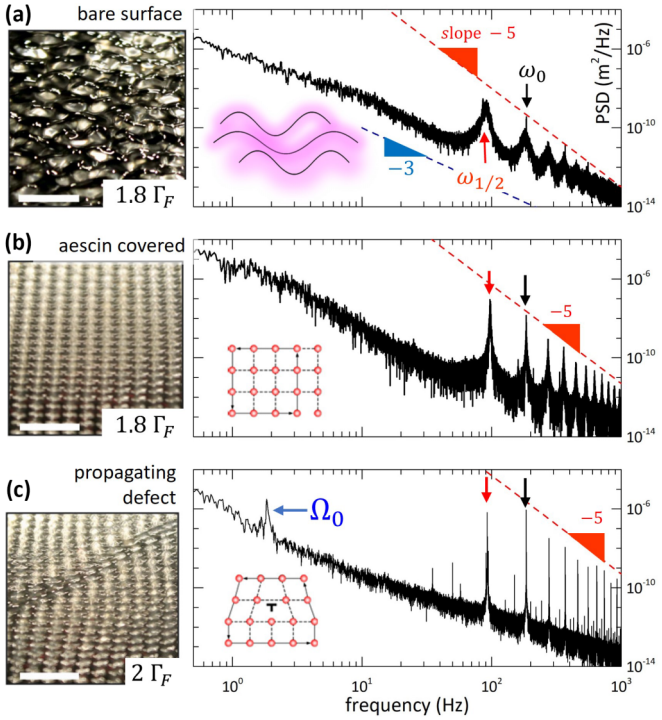

FIG. 1. Hydrodynamic crystal and dislocation mode. Discrete surface waves in the capillary Faraday wave (FCW) domain ($\omega_0 = 185$ Hz $\gg \omega_{cap}$) at $\Gamma > \Gamma_F \approx 0.2$ (left panels; approximate scale 5 mm). Wave field spectral densities detected by LDV as discrete cascades of harmonics $\omega_n = n\omega_0$, of the fundamental mode ω_0 (black arrow, right). They decay at inertial scaling (PSD $\equiv P_{\psi\psi} \propto \omega^{-5}$, red), including the Faraday subharmonic ($\omega_{1/2} = \omega_0/2$; red arrow) and overtones ($\omega_{n/2} = n\omega_{1/2}$). Brownian randomness is evident in the noisy background (friction-filtered ω^{-3} decay; blue); see (Ref. [11]) for details. (a) Disordered (incoherent) FCWs in a bare water surface ($1.8\Gamma_F$). (b) HC lattice based on coherent FCWs in an adsorbed layer of aescin (0.4 m*M*), same conditions as in (a). An organized FCW field emerges as a square lattice for which the spectral peaks narrow. (c) Lattice excitation as a propagating line defect (at $2\Gamma_F$); a dynamic peak appears at $\Omega_0 = 1.8$ Hz $\ll \omega_0$.

In this work, we use the intrinsically frozen HCs to study lattice defects, single and collective, as the breakdown route for crystal disorder and further melting upon excitation. Figure 1 highlights the resonant FCW instability, genuinely subharmonic, guiding two opposite lattice processes: first, HC freezing upon coherent wave field focusing on low energies [Figs. 1(a) and 1(b)], then lattice dislocations through defocusing at higher energies [Fig. 1(c)]. These solid-like interactions pertain to a flexural FCW domain, frozen under intrinsic shear stiffness [11]. Our previous results demonstrated FCW-field self-focusing essential for HC freezing as an organization of the discrete nonlinear modes in a structured lattice [11]. So far, wave decoherence mechanisms, like defocusing and phase unlocking, have not been analyzed considering material components, such as inertia, surface elasticity, and friction. However, these factors are crucial in explicitly breaking symmetries within the discretely generating wave field [10,29]. We analyze lattice disorganization through single-line defects emerging among nonlinearly halved FCW modes, akin to Taylor dislocations apppearing in microscopic crystals under mechanical stress or heat [30]. Although some symmetry breakdowns have been studied using granular matter [23], and in bounded realizations under frictional control [15,31], collective lattice instabilities leading melting mediated by lattice defects on HCs have not been reported hitherto.

The paper is divided into two complementary parts, combining experiments and theory to explore fluid matter components, symmetries, and interactions involving self-focused FCW lattices leading to ordered HC freezing and disordering counterparts e.g., crystal distortion and melting. First, we present experiments that highlight the FW behavior of freestanding square HC lattices, stabilized by intrinsic surface stiffening, in both steady-frozen states and during the dynamic transition to chaotic melting. Second, we introduce a nonlinear field theory (Landau-Ginzburg) that explains those processes driven by massive FCW interactions under parametric resonance. We discuss the experimental findings within a matter-wave theoretical framework considering Faraday (wave-halving) instability, which creates HC order through coherent self-focusing and induces disorder under symmetries broken among massive modes. We summarize our conclusions, adopting the matter-wave perspective, extending this notion to the discrete and coherent FCW packets representing correlated fluid elements arranged as HCs in two dimensions.

II. EXPERIMENT

To excite discrete, nonlinear FCW fields, we followed the same rationale as described in Ref. [11]. Briefly, CWFs emerge as frequency-halving resonances from a fundamental driving frequency (ω_0), above a critical acceleration (a_F) (see the Supplemental Material, Fig. S1 [32]) [9,10], and in cylindrical vessels $a_F \approx 8\mu(\rho/\sigma)^{1/3}(2\pi\omega_0)^{5/3}$ (fluid characteristics: μ kinematic viscosity; ρ density; σ surface tension) [33]. Vertical vibration was driven with an acoustic speaker powered at a single frequency ω_0. Upon monochromatic power $A(t) = A_0\cos(\omega_0 t)$, the FW field appears with amplitude $\psi_0 \propto A_0$, under liquid acceleration $a_0 \equiv A_0\omega_0^2 \geqslant a_F$. Relative to the acceleration of gravity (g), the reduced driving parameter $\Gamma \equiv a_0/g$ is varied along the FCW interval [$\omega_0 \geqslant \omega_{cap} = (4\rho g^3/\sigma)^{1/4} \approx 15$ Hz]; for water at room temperature, $\Gamma \geqslant \Gamma_F(\equiv a_F/g) \approx 0.2$ [10]. Accordingly, container vessels were chosen with dimensions larger than the fundamental FCW length, i.e., $L \gg \lambda_F \approx 2\pi(\sigma/\rho\omega_0^2)^{1/3}$ [10,33]. No gravity waves were further considered (at $\omega < \omega_{cap}$). To realize HCs on highly tensioned water surfaces ($\sigma \approx 0.07$N/m), we used the soluble surfactant β-aescin, a shear-stiffening agent able to self-focus the surface FW field [11]. Since requesting intrinsic rigidity higher than surface tension ($G \gg \sigma$) (Supplemental Table T1 [32]), HC realizations are formed stable, reformable, and tunable along a reversible FCW freezing-melting scenario (Supplemental Movie M1 [32]).

III. FCW DISPERSION

We analyzed phenomenological $\lambda_F - \omega_0$ plots (Supplemental Fig. S2 [32]). In bare surfaces ($G = 0$), disordered

FCWs followed Kelvin's (liquidlike) dispersion law $\omega_C^2 \approx \sigma k^3/\rho$, with higher wave vectors k, resulting in faster velocities due to surface fluidity [20]. Adding surface-rigidizing aescin ($G \gg 0$) transformed FCWs both structurally, by ordering HCs upon, and dynamically, by turning them dispersionless (solidlike), as acoustic "crystal waves" in a regular lattice [30]. Specifically, 0.4 mM aescin decreased surface tension ($\sigma \approx 0.04$N/m), enhancing surface hardness ($G \approx 1\text{N/m} \gg \sigma$), upon freezing with sufficient surface stiffening $\kappa \equiv G/\sigma \gg \kappa_{fr} \approx 2$, as determined experimentally [11]. Stable, squared HCs were obtained above the capillary frequency ($\omega \geqslant \omega_{cap}$), resulting in FW lattices with C_4 symmetry [30] (Supplemental Fig. S3 [32]), as based on three-wave resonant coupling [10,12]. These squared HCs established a conservative FCW field mastered by the fundamental Faraday wave $\omega_0/2 = c_F k_F$ [10,29], characterized by locked phase at constant velocity $c_F \approx (G/\rho h)^{1/2} = 0.35 \pm 0.02$m/s [30] (taking $G \approx 1$N/m, $\rho \approx 1\text{g/cm}^3$, an effective thickness is estimated compatible with wave field amplitude $h \approx \psi_0 \approx 1$ cm). In other words, HCs are coherent crystal waves (self-focused) in ordered lattices with a unit cell size $a \equiv \lambda_F = 2\pi/k_{1/2}$.

IV. LASER DOPPLER VIBROMETRY (LDV): FCW SPECTRUM AND PHASE SPACE

The surface wave field $\psi(\mathbf{r}, t)$ was analyzed by laser Doppler vibrometry (LDV), measuring the velocity $\dot{\psi}(t)$ detected in a surface emplacement at phase lock-in with the driving signal A(t). Vertical displacements are obtained by stepwise integration $\psi(t_{i+1}) = \psi(t_i) + \dot{\psi}(t_i)\Delta t$ (Δt being the time step); we compute the power spectral $\text{PSD}(\omega) \equiv P_{\psi\psi} \equiv \int |\psi(t)|^2 e^{-i\omega t} dt = P_{\dot{\psi}\dot{\psi}}/\omega^2$ (Fig. 1, right). Because of natural stochasticity, we cannot plot deterministic position-velocity portraits ($\psi - \dot{\psi}$). Instead, we charted as phase portraits the densities of states explored along the time series (PDFs). The statistical energy landscape approached the Gibbs distribution $U/k_BT \equiv -\ln(\text{PDF})$. To calculate systemic circulations as probability currents in phase space, we exploited statistical bootstrapping methods developed to detect broken detailed balance in complex systems [34].

V. HC FREEZING

FCW fields appeared as a superposition of two spectral cascades ($\psi \equiv \psi^{(0)} + \psi^{(1/2)}$) (Fig. 1, right): the ordinary harmonic (o) led by the fundamental mode (ω_0) and the extraordinary subharmonic (e) following the Faraday halving excitation ($\omega_{1/2} \equiv \omega_0/2$) [10,11]. Both decay at parametric resonance $P_{\psi\psi} \sim F_0^2/\omega_{o,e}^5 \sim \Gamma^2\omega^{-5}$, akin to a nonlinear oscillator (NLO, Duffing-like) restored by inertia under quartic stiffness and frictional dissipation (Supplemental Note N1 [32]) [11,29]. Hence the NLO modes are relatively broad in the dissipative liquidlike regime [Fig. 1(a)] and become sharply defined in the highly stiffened solidlike regime [Fig. 1(b)]. In aescin-stiffened water surfaces ($\kappa \equiv G/\sigma \gg \kappa_{fr} \approx 2$), just above the Faraday threshold ($\Gamma \geqslant \Gamma_{fr} \approx 1.8\Gamma_F$), we excite square lattices of planar FCWs (C_4 symmetry). Obviously, HCs are nonequilibrium structures unable to form spontaneously in the absence of the pilot FCW field (at $\Gamma < \Gamma_{fr}$). Hence HCs were considered at a reference state $\omega_0 = 175$ Hz, well above the capillary frequency to avoid gravity effects ($\omega_0 \gg \omega_{cap}$); here, the ordered FCWs resonate with oscillating bulk inertia giving rise to a distinctive FW subharmonic ($\omega_{1/2} = 87.5$ Hz) with a fundamental wavelength ($\lambda_{1/2} \approx 1.03$ mm) (Supplemental Fig. S3 [32]). Not only for the chosen reference Ω_0 state, but systematically across the FCW domain (Supplemental Fig. S4 [32]), we found squared HC lattices with unit cells smaller than the vessel dimensions ($\lambda_{1/2} \ll L$). No boundary constraints nor meniscus effects were relevant in the FCW/HC setup [11].

As a rule of thumb, Fig. 1 illustrates HCs primarily distorting through Taylor-like dislocations appearing along principal lattice axes (see also Supplemental Movie M2 [32]). Likewise, progressive energy injection elicits newly excited FCW subharmonics as mobile line defects, leading to phase defocusing and collective distortion (Supplemental Movie M3 [32]), and eventually to chaotic crystal melting (Supplemental Movie M4 [32]). Without aescin added, the FWs appeared to be surface disordered (at $\Gamma = 1.8\Gamma_F$). At $1.8\Gamma_F$ forcing, the presence of aescin "freezes" the FCWs into square HCs, forming regular lattices under wave field self-focusing [Fig. 1(b), left] [11]. Characteristic FW spectral features are preserved in this focused state, showing evident peak narrowing as crystal order increases [Fig. 1(b), right] [11]. A weak energy increase ($2\Gamma_F$), elicits a single dislocation to appear (Taylor-like), causing mobile lattice distortion [Fig. 1(c), left]. This excitation is spectrally identified as a slow propagating mode $\Omega_0 \approx 1.8$ Hz $\ll \omega_{1/2}$ [Fig. 1(c), right]. Therefore, we analyze the FCW-interaction phenomena in a unified mean-field theory describing Faraday interactions responsible for both freestanding HC formation, and intrinsic disorder instabilities towards turbulent melting [21].

VI. HC LATTICE PHENOMENA: INTRINSIC FREEZING AND DISORDER MEDIATED BY DEFECTS

Figure 2 shows an experimental sequence of tunable FCW fields leading to freestanding HC lattices with a relatively large unit cell (for a $\geqslant L$). Even if framed in a circular boundary, these low-frequency FCW/HCs do preserve the square C_4 symmetry (Supplemental Fig. S5 [32]). They span from disordered FCWs (liquidlike), leading to HC freezing (solidlike), up to the molten crystal state (fluid), through lattice excitations (disordering). A nontrivial dynamics is evidenced from systemic probablity circulations (Fig. 2, lower panels). Disordered FCWs behave like a delocalized Duffing NLO [Fig. 2(a)], while ordered HCs exhibit centripetal dynamics typical of a locked resonator [Fig. 2(b), HC-0 ground state] [10,29]. As the HCs become distorted, lattice dynamics evolve from slight centrifugal trends to more pronounced external orbits in a weakly defocused field (slightly excited crystal; exc-HC at $2\Gamma_F$). This reversible progression follows peripheral orbiting under increased field defocusing (distorted lattice at $6\Gamma_F$, dist-HC). Finally (at $\Gamma \geqslant 8\Gamma_F$), the system reaches a molten state dominated by frictional penalties on fast motions [Fig. 2(c)]; here, the largest wave height occurs at the slowest velocity.

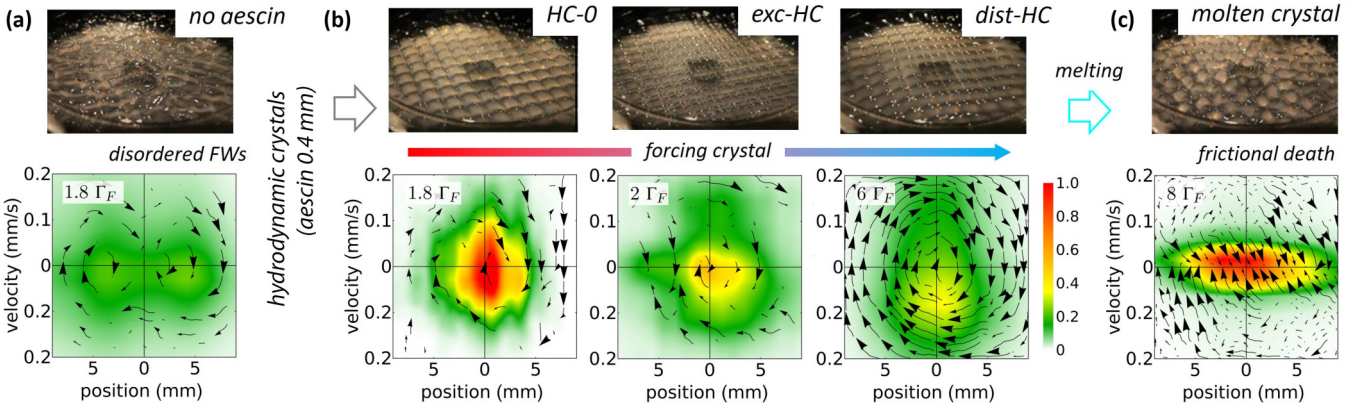

FIG. 2. FCW-field states and phase-space currents: (a) Disordered FCWs with defocused dynamics. (b) Square HCs at variable degrees of lattice distortion; HC-0: Zero-energy state, near-perfect crystal in a focused field promoting resonant orbits around the ground state; exc-HC: excited state with nascent dislocations from field defocusing; dist-HC: distorted lattice with collective excitations leading peripheral resonant dynamics. (c) Molten crystal under frictional death. Let us notice the freestanding character of the FCW/HC structures with a square capillaritylike geometry in a circular container of relatively small size ($L = 5$ cm; $a \equiv \lambda_F \approx 0.4$ cm; $\omega_0 = 40$ Hz $> \omega_{\rm cap}$).

VII. PROPAGATING DEFECTS AND COLLECTIVE DISTORTIONS

Figure 3 shows LDV spectra measured for the reference state ($\omega_0 = 175$ Hz) at distinct stages of lattice distortion (see also Supplemental Fig. S5 [32]). Single dislocations appear only at small deformations just above the freezing point [$\Gamma \approx 2\Gamma_F \gtrsim \Gamma_{\rm fr}$, Fig. 3(a)], exhibiting propagative characteristics indicative of material elasticity enabled by in-plane stiffness. The natural dislocation frequency is fixed by lateral surface rigidity $\Omega_0 \cong (G/h^3\rho_s)^{1/2}$, ρ_s being a surface mass density. Given $\Omega_0 \approx 1.8$ Hz, we estimate $\rho_s \approx 8{\rm g/cm}^3 \gg \rho$ (for $G \approx 1{\rm N/m}$), representing a highly massive layer of thickness $h = \rho_s/\rho \approx 1$ cm, comparable to wave dimensions ($h \approx \psi_0 \geqslant \lambda_{1/2}$). Well above the freezing point (at $4\Gamma_F$), we still detect the fundamental dislocation peak (Ω_0), followed by a cascade of harmonics ($2\Omega_0,\ 3\Omega_0, \cdots$), with a scaling structure resembling the Faraday resonance [ω^{-5} inertial decay over an ω^{-3} frictional background, Fig. 3(b), left]. Here, the crystal dislocations self-organize into a collective lattice distortion with a wavelength $\Lambda \approx 3.2$ cm ($Q \equiv 2\pi/\Lambda \approx 2\ {\rm cm}^{-1}$), effectively a massive spatial modulation ($\Lambda = N\lambda_{1/2}$, spanning at least $N \approx 18$ unit cells (Fig. 3, right). Assuming crystal homogeneity, we estimate the massive mode propagating at a constant velocity $c_\Omega \equiv \Omega_0/Q \approx 10^{-2}{\rm m/s} \ll c$, slower than lattice-wave phase velocity ($c_F \approx 0.3$ m/s), which is consistent with the visual observation (Supplemental Movie M3 [32]). Additional forcing (at $6\Gamma_F$) caused collective excitations with a canonical Faraday o/e structure: ordinary harmonics $\Omega_n = n\Omega_0$ and extraordinary subharmonics $\Omega_{n/2} = n\Omega_{1/2}$, both emerging from the fundamental resonance $\Omega_{1/2} = \Omega_0/2 \approx 0.9$Hz [Fig. 3(c), left]. These strong lattice distortions appear as collective defect modulations [Fig. 3(c), right], akin to an inertial Faraday resonance causing massive oscillatory lattice distortions (Supplemental Movie M5 [32]). We emphasize the progressive halving nature of these collective lattice excitations (nonlinear $\Omega_{n,n/2}$, phononlike), whose early signature appeared from the single-line dislocations propagating at Ω_0. Further forcing at $8\Gamma_F$ causes structural disorder to spectrally superpose as a Landau spectral continuum (above the critical amplitude $\Gamma_{\rm crit} \approx 7\Gamma_F$), compatible with the frequency-halving instability associated with fluid turbulence [20,21]. Peak broadening, mode superposition, and the shift from inertial scaling to frictional decay characterize this "molten" FCW state [Fig. 3(d), left], with steady "liquid" capillary waves becoming turbulent [Fig. 3(d), right]. These resonant behaviors are consistently reproduced under different excitation conditions (ω_0 and Γ relative to Landau's critical onset of fluid turbulence Γ_F), with solidlike lattice defects and liquidlike dynamics appearing underneath. On the one hand, the structural mode appears nondispersive in the low forcing domain ($\Gamma \lesssim 7\Gamma_F$) i.e., $\Omega_0 = c_\Omega Q$, with a constant propagation velocity $c_\Omega = 1.1 \pm 0.1{\rm cm/s}$ [Fig. 3(e)], consistent with above estimates. On the other hand, dissipation becomes evident at high forcing ($\Gamma \gtrsim 7\Gamma_F$), as all spectral peaks broaden due to Γ-induced unsteadiness [Fig. 3(f)]. The most ordered crystal, identified by sharp spectral peaks (at $\Gamma_{\rm fr} \approx 1.8\Gamma_F$), becomes progressively broader during melting. The chaotic molten crystal exhibits liquidlike unsteadiness akin to a bare water surface [Fig. 3(f)]. Expanding on Landau's conjecture for chaotic turbulent flow [20,35], we propose that this intrinsic unsteadiness is essential for HC melting via lattice breakdown (Supplemental Movie M3 [32]).

VIII. HC FIELD THEORY: POTENTIAL ENERGY

Figure 4(a) shows energy landscapes based on experimental PDFs calculated for reduced displacements $\psi \to \psi/\psi_0$. Different interactions and symmetries in the FW formation were revealed in representative scenes (at $\Gamma \geqslant \Gamma_F$), ranging from (left to right) disordered fluid of unfocused FCWs without rigidizing aescin ($\Gamma < \Gamma_{\rm fr}$, $\kappa \approx 0$), hydrodynamic crystal under aescin-induced surface stiffening (at $\Gamma_{\rm fr} \approx 1.8\Gamma_F$, with $\kappa > \kappa_{\rm fr}$), emergent crystal dislocations (at $\Gamma \geqslant 4\Gamma_F$), and crystal melting into a turbulent fluid above the critical Landau's threshold (at $\Gamma \geqslant \Gamma_{\rm crit}$). From a field theory perspective, considering these symmetries [36], the potential energy

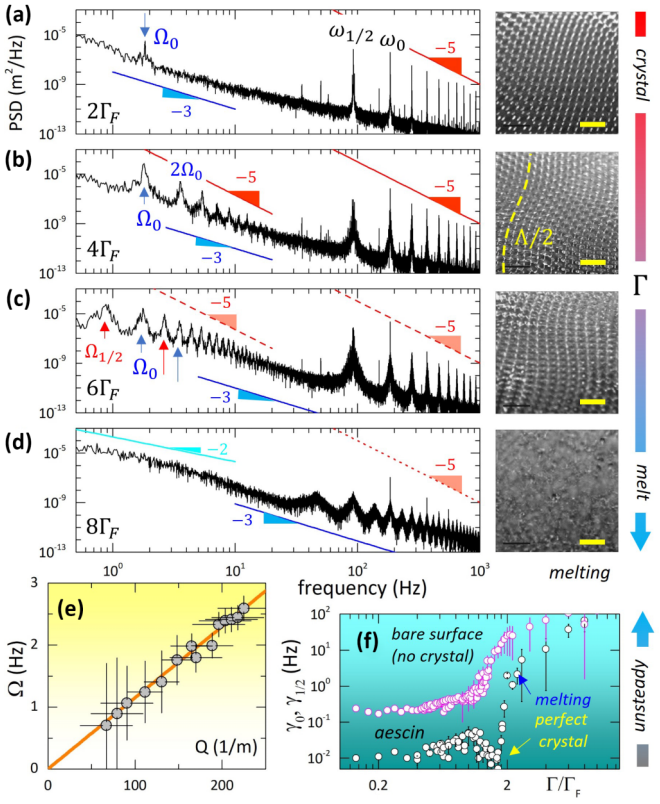

FIG. 3. Crystal melting under collective lattice excitation. HCs distorted upon increasing forcing (Γ): Left: LDV spectra. The FCW field appears as a nonlinear cascade from the natural frequency ($\omega_0 = 185$ Hz). The (sub-) harmonic decay is governed by inertia ($\sim\omega^{-5}$). The spectral background is limited by friction ($\sim\omega^{-3}$). Straight lines represent expected scaling; dashed lines are guides for the eye for vanishing behavior. Structural distortions do appear in the low-ω band. Right: Real lattices (scale bar 5 mm). (a) Weakly distorted square lattice at $2\Gamma_F$, with single dislocations propagating at $\Omega_0 \approx 1.8$ Hz. (b) Collective lattice modes at $4\Gamma_F$; composed by an inertial o cascade ($\sim\Omega^{-5}$), of structural modes (fundamental Ω_0, and higher harmonics $2\Omega_0, 3\Omega_0, \cdots$, left), causing collective lattice distortion of wavelength Λ (right). (c) Distorted lattice at $6\Gamma_F$. The collective mode undergoes frequency halving at $\Omega_{1/2} \approx 0.8$ Hz $\approx \Omega_0/2$, with extraordinary cascade at $n\Omega_{1/2}$, superposed to ordinary cascade at $n\Omega_0$. (d) Molten crystal at $8\Gamma_F$. Through effective frequency-halving bifurcation, low-frequency surface distortions broaden spectral peaks, resulting in a continuous spectrum known as Landau's turbulence spectrum ($\sim\omega^{-2}$). (e) Dispersion relation for the structural mode. Symbols: experimental data; straight line: linear fit to nondispersive relationship. (f) Γ dependence of spectral unsteadiness measured as peak widths for fundamental mode (γ_0); Faraday subharmonic ($\gamma_{1/2}$). Experimental series: bare surface (magenta); HC (white).

expands as a generalized NLO potential:

$$U(\psi)/U_0 = k\psi^2/2 + \alpha\psi^3/3 + \beta\psi^4/4 + \delta\psi^6/6. \quad (1)$$

Here, k is a dimensionless spring constant representing the harmonic FCW force governed by surface tension, with anharmonic couplings α, β, and δ from surface-intrinsic interactions. Zeroth-level energy $U_0 \equiv k\psi_0^2/2$ determines the normalization constant at forcing amplitude $F_0 = k\psi_0$, i.e., $U_0 = F_0\psi_0/2$. Relevant timescales are based on the fundamental frequency (ω_0), with $k \equiv \sigma_{eff}/m\omega_0^2$ and $\beta \equiv G_{eff}/m\omega_0^2$, defined in terms of effective surface stiffnesses (σ_{eff} and G_{eff}) and inertial mass ($m \equiv F_0/A_0\omega_0^2$) [11]. Due to rotational invariance (fluidity), the vacuum state maintains parity symmetry and is characterized by a harmonic response $k > 0$, plus quartic coupling $\beta > 0$ [10]. This fluidlike state encodes the FCW interaction [10,11,29], as well as the nonlinear (three-wave) generation through direct field self-interaction $\psi^2 \mapsto \varphi$ [40]. False vacuum states indicate effective fluid metastability ($k < 0$) [37]. The quartic structure translates the square-lattice C_4 symmetry into an equivalent harmonic FCW field; if $\varphi = \sqrt{2}\psi^2/2$, we cast $U_\beta = \beta\psi^4/4 \mapsto k_\beta\varphi^2/2$ upon quartic spring constant $k_\beta \equiv \beta$ [11,36]. The stiffening parameter is redefined as $\kappa \equiv \beta/k \Rightarrow G/\sigma$. Parity symmetry is lost under cubic coupling ($\alpha \neq 0$). In order for stable vacuum to happen, a bounding term is introduced ($0 < \delta < |\beta|$), enabling surface integrity through mean-field confinement.

IX. HC FIELD: SYMMETRIES

The disordered FW liquid (at $\Gamma \geqslant \Gamma_F$ and low κ) is characterized by a slightly repulsive harmonic response ($k \lesssim 0$) and marginal quartic nonlinearity under Faraday resonance $U \approx U_L \approx k\psi^2/2(1 + \kappa\psi^2/2)$ (Fig. 4(a), left). However, at $1.8\Gamma_F \approx \Gamma_{fr}$, hydrodynamic crystal freezing occurs as the FCW field self-focusses under relevant stiffening ($\kappa \gg 1$). Above the freezing point ($\kappa > \kappa_{fr} = 2$), with sufficient driving force higher than capillary $F_0 > F_{fr} = 3(2k^3/\beta)^{1/2}$ (at $U_\beta > U_L$), the ground HC state holds $U_{HC}^{(0)} \approx U_L + \beta\varphi^2/2$; for the real hydrodynamic crystal, we estimate $\kappa \approx 20 \gg \kappa_{fr}$ [Fig. 4(a)], second panel). At $4\Gamma_F$, collective lattice distortion occurs due to explicit symmetry breaking [Fig. 4(a), third panel]. Here, HC field parity is broken by cubic excitation, with $U_{HC}^{(exc)} \approx U_{HC}^{(0)} + \alpha\psi^3/3$ (for $\alpha^2 \geqslant 4k\beta \gg 0$). This represents the structural mode Ω_0 (and relative Ω_n) shifting to $\psi_0^{(exc)} \approx -\alpha/\beta$ in an effectively focused spring $k^{(exc)} \approx k + \alpha^2/\beta$, with enhanced nonlinear stiffness $\beta^{(exc)} = \beta + 2\alpha/3$ [35]. At $8\Gamma_F$, the HC field becomes completely defocused under repulsive quartic interaction [HC field softening at $\beta \ll 0$; Fig. 4(a), right]. Here, the molten lattice becomes more stable, as a disordered liquid ($U_{melt} < U_{HC}$), although potentially unsteady [Fig. 3(f)].

X. EQUATION OF MOTION: RIGIDNESS-HARNESSED NLO DYNAMICS IN A PARAMETRIC RESONATOR

Inspired by the Kolmogorov-Zakharov-Filonenko (KZF) theory for capillary wave turbulence [38,39], surface stiffness is proposed to form the dynamic framework for FCW condensation [11]. The KZF field determines the spatial structure imposed by Laplace stresses (curvature-surface tension) and the three-wave colliding kinetics described by the nonlinear Schrödinger (NLS) equation [40],

$$i\psi_t + k\nabla^2\psi + \beta|\psi|^2\psi = 0, \quad (2)$$

which describes nonlinear, inviscid surface propagation by CW genesis under three-wave couplings [20]. This Partial differential equation accounts for Laplacian symmetries likely

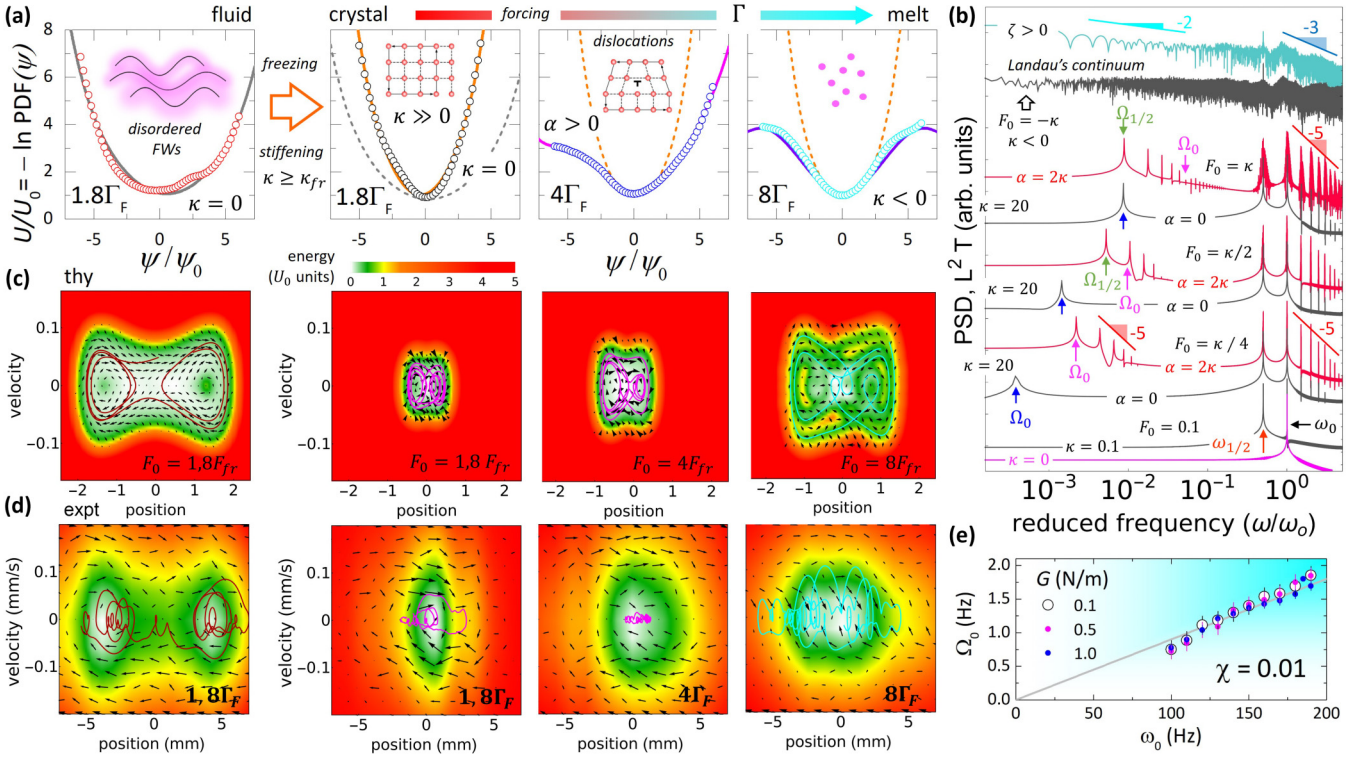

FIG. 4. Energy landscapes and Duffing-NLO dynamics. (a) Potential energy in representative states (experimentally inferred as $U/U_0 = -\ln(PDF)(\bar{\psi})$ for $\bar{\psi} = \psi/\psi_0$; normalization $U_0 = -\ln(PDF_{max})$ and $\psi_0 = 2$ mm). Symbols: experimental data. Straight lines: best fits to the NLO potential in Eq. (1) (disordered FCWs: $k = -0.1$, $\kappa = 1.1$, $\alpha = 0$; near-ordered crystal $k = 1$, $\kappa = 19.8$, $\alpha = 0$; distorted crystal $k = 1$, $\kappa = 19.9$, $\alpha = 40.3$; molten crystal $k = 0.9$, $\kappa = -3.2$, $\alpha = 0$; 10% typical uncertainty; reduced units referred to $m = 1$). All NLO potentials are corralled by a perimetric wall as $U = U_{NLO} + \delta\bar{\psi}^6$ ($\delta < 1$), which accounts for effective surface confinement ($U \approx U_{NLO}$ for $|\bar{\psi}| < 1$ and $U \to +\infty$ for $|\bar{\psi}| \gg 1$). (b) NLO spectra at increasing force F_0 [NLO parameters inferred from (a)]. Main parametric resonance features are predicted including Faraday field $\psi^{(0)}U\psi^{(1/2)}$, and modulation modes Ω_n. (c) Theoretical phase portraits for the NLO resonator at representative states [same potentials as in (a)]; forcing amplitude F_0 by reference to $F_{fr} = k\psi_0$). A representative trajectory during a $10^3/\omega_0$ cycle is snapshooted over the calculated energy landscape. Arrows indicate global circulations in phase space. (d) Experimental phase portraits for the corresponding FW status [same symbols as in (c)]. (e) Experimental lattice susceptibility for the HC collective modes at variable surface stiffening. Straight line: best fit to a linear dependence for amplitude modulation modes.

imposed by governing surface tension [20]. However, NLS dynamics lacks the momentum term needed for the FW field under parametric resonance [10,29]. Assuming NLS compatibility with the Stokes flow in FCW excitation, we propose a minimal, comprehensive NLO with a forced field ODE structure derived from Eq. (1). Under homogeneous forcing and viscous dissipation, we reformulate the wave field equation of motion as

$$m\psi_{tt} + \zeta\psi_t + k\psi + (\alpha + \beta\psi + \delta\psi^3)\varphi = F(t). \quad (3)$$

This NLO-Duffing generator enables Faraday resonances between wave inertia (represented by the inertial mass m) and the monochromatic driving source $F(t) = F_0\cos(\omega_0 t)$. It drives a spatially homogeneous, time-discretized response $\psi = \psi^{(0)} + \epsilon\psi^{(1/2)}$, composed of main lattice wave field $\psi^{(0)}$ led by the natural oscillatory response $\omega_0 = (k/m)^{1/2}$, and subsidiary ($\epsilon < 1$) subharmonic field $\psi^{(1/2)} \propto \psi^2 \mapsto \varphi$, bifurcating under parametric resonance at self-interaction, i.e., $\ddot{\varphi} = -\omega_{1/2}^2(\psi + \alpha/\beta)\varphi$ [6,21]. The resonant half-harmonic $\omega_{1/2}^2 = \beta/m_{1/2}$ arises from quartic stiffening ($\beta > 0$), generating FCW packets of mass $m_{1/2}$. Since $\omega_{1/2} \equiv \omega_0/2$, thus $m_{1/2} \equiv 4m\kappa$, meaning field stiffening effectively increases φ inertia. The kinetic term assimilates to a generalized drag with a complex friction coefficient $\zeta \equiv \zeta_{visc} + i\omega_0 m$; in the inviscid case ($\zeta_{visc} = 0$) it reduces to the inertial NLS structure ($\zeta = i\omega_0 m$). This basic NLO dynamics matches observed phenomena [11], particularly, inertia-driven Faraday ω^{-5} cascades and ω^{-3} frictional background [11]. Generalized frequency and phase locking, frequency halving, and systemic discretization are also predicted as NLO-FCW features essential for the Faraday bifurcation forming the squared HC (see Supplemental Materials in Ref. [11]). Understanding these collective massive excitations under Faraday instability is crucial for studying crystal melting.

XI. COLLECTIVE EXCITATION: HC SYMMETRY BREAKING

Figure 4(b) shows NLO predictions in agreement with experimental spectra (Fig. 3). At $\kappa \gg \kappa_{fr}$, the parent o cascade $\psi^{(0)}$, as well the FW-resonant extraordinary field $\psi^{(1/2)}$, appear both as intercoupled HC field generators [Fig. 4(b), lower panels]. Above the freezing point ($F_0 > F_{fr}$), a structural excitation emerges as a NLS-modulation instability [41,42], appearing as a nondispersive, massive collective resonance

of subharmonic frequency $\Omega_{1/2} = \Omega_0/2 \equiv (k/M)^{1/2} \propto \omega_0$, where $M \equiv \rho\Lambda^2 h \Leftrightarrow \rho_s h^3$ is reinterpreted here as the total inertial mass of a collective disordering excitation (Supplemental Movie M5 [32]). In line with the cubic asymmetry appreciated in distorted lattices [Fig. 3(b)], a structural Ω_n cascade appears when parity is explicitly broken ($\alpha > \beta \gg 0$). Effective stiffening occurs then ($\beta^{(\mathrm{exc})} > \beta$), and secondary resonances refocus within this excited state. Consequently, additional NLO forcing causes $\Omega_{n/2}$ halving from such an odd α-perturbed state akin to collective distortions in real lattices [Fig. 3(c)]. At high forcing, Landau's continua are predicted in defocusing potentials ($\kappa < 0$), indicating symmetry losses during the melting transition [43]. NLO-Duffing-like friction also limits unsteadiness, especially at high energy [Fig. 4(b), upper]. Figure 4(c) shows theoretical phase portraits in their energy landscapes, serving as ODE-NLO predictors compatible with peripheral orbiting observed in real lattices [Fig. 4(d)]. Even with noise, trajectories focus under lattice freezing and defocus under symmetry distortion (Supplemental Movies M6–M9 [32]). These simulations highlight quartic self-interactions as key ordering-disordering factors governing the Faraday-halving bifurcation from frozen crystal to molten fluid.

Collective lattice distortion and eventual melting occur as explicit symmetry breaking from the ground crystal state upon collective Faraday excitation [Figs. 4(c) and 4(d)]. The inertial and massive nature of these distortions is evident as the dislocation modes propagate without dispersion [Fig. 3(e)]. They appear as modulation modes under inertial control [11], emerging at frequency $\Omega_0 = \chi\omega_0$, determined by the unit cell size (fixed by ω_0) through a lattice susceptibility χ [30]. Figure 4(d) presents experimental data for different shear rigidities above the freezing point ($G \geqslant G_{\mathrm{fr}} \approx 0.1\mathrm{N/m}$). The results indicate a common susceptibility $\chi = 0.010 \pm 0.006$, independent of surface freezing and external forcing.

From a matter-wave perspective, the FW packets are located at the lattice nodes as pseudoparticles with inertial mass concentrated over their wavelength [11]. Collective distortions stem from these FCW packets, appearing as massive excitations that explicitly break lattice symmetry (density waves as pseudo-Goldstone lattice modes) [24,44]. They span a collective wavelength $\Lambda = N\lambda_{1/2}$, and comprise a total mass $M_G = N^2 m_{1/2}$, involving inertial resonance under surface density $\rho_s \equiv M_G/\Lambda^2 \equiv m_{1/2}/\lambda_{1/2}^2$. Given the propagating nature $\Omega_0^2 = (G/h\rho_s)Q^2$, since $m_{1/2} = 4mG/\sigma$, then $\Omega_0 = \pi\omega_0/N^2$, and we deduce a conserved susceptibility $\chi = \pi/N^2$. For the observed $N \approx 18$ (Fig. 3), one estimates $\chi \approx 0.01$ in agreement with experiments [Fig. 4(e)]. As in classical crystals, this collective phonon arises from defect size and lattice broken symmetry (Supplemental Movie M5 [32]), not from particular stiffness nor from the crystal size requested [30].

XII. CONCLUSIONS

As a fundamental principle, the ground crystal state arises from the capillary-Faraday wave (FCW) interaction intrinsically self-focused by surface stiffening. Together with bulk inertia, this interaction creates the discrete resonances necessary to crystallize the FWs into coherent packets, or pilot waves, localized in a regular lattice of particulate fluid matter. Our study shows crystal defects appearing as slow lattice modulations that result from bifurcated FW resonances (Taylor dislocations). Since energy is finite under these single excitations, lattice symmetry is explicitly broken by the collective distortions caused by the local reorientation of parity symmetry, favoring one dislocated direction in the crystal. Further cooperation among multiple halved modes is intercoupled by the Faraday interactions (collective modes). These massive, cooperative excitations become collective modes (phononlike) among the discrete, coherent, and momentum-containing FCW packets, effectively carrying the material "atoms" that form the hydrodynamic crystal, either in a frozen configuration, or further distorted by deformation or "heating" (i.e., forcing).

To summarize, we have demonstrated macroscopic two-dimensional (2D) realizations of ordered and distorted hydrodynamic crystal lattices engendered by the Faraday bifurcation, appeared as a frequency-halving resonant interaction. Above the freezing point of the ordered crystal, lattice order is progressively lost under excitation through disorganizing dislocations that propagate under explicit symmetry breaking, akin to lattice vibrations (phonons) in classical crystals. These collective distortions, originating from the parent FW lattice, dominate the dynamic pathway towards crystal melting with a consistent Faraday hierarchy modulated by explicit broken symmetries. As the distorted crystal transitions to a chaotic molten fluid appear, these secondary instabilities progressively halve, creating a continuum of disordered states reminiscent of Landau's picture of nascent turbulence. This study introduces a matter-wave paradigm for collective 2D-lattice excitations as the natural route for hydrodynamic crystal melting, establishing a macroscopic laboratory for testing inflationary dynamics under systemic FW halving bifurcation.

ACKNOWLEDGMENTS

This work was supported by the Spanish funding agencies Ministerio de Ciencia, Innovación y Universidades—Agencia Estatal de Investigación (AEI) under Grants No. PID2019-108391RB-I00 and No. TED2021-132296B-C52, and Comunidad de Madrid under Grants No. Y2018/BIO-5207 and No. S2018/NMT-4389.

[1] P. W. Anderson, More is different. Broken symmetry and the nature of the hierarchical structure of science, Science **177**, 393 (1972).

[2] P. D. Fleming and C. Cohen, Hydrodynamics of solids, Phys. Rev. B **13**, 500 (1976).

[3] D. Ruelle, Smooth dynamics and new theoretical ideas in nonequilibrium statistical mechanics, J. Stat. Phys. **95**, 393 (1999).

[4] R. Dreyfus, P. Tabeling, and H. Willaime, Ordered and disordered patterns in two-phase flows

in microchannels, Phys. Rev. Lett. **90**, 144505 (2003).
[5] T. Beatus, T. Tlusty, and R. Bar-Ziv, Phonons in a one-dimensional microfluidic crystal, Nat. Phys. **2**, 743 (2006).
[6] A. V. Andreev, S. A. Kivelson, and B. Spivak, Symmetry and symmetry-breaking bifurcations in fluid dynamics, Annu. Rev. Fluid Mech. **23**, 341 (1991).
[7] M. C. Cross and P. C. Hohenberg, Pattern formation outside of equilibrium, Rev. Mod. Phys. **65**, 851 (1993).
[8] J. P. Gollub and J. S. Langer, Pattern formation in nonequilibrium physics, Rev. Mod. Phys. **71**, S396 (1999).
[9] M. Faraday, On a peculiar class of acoustical figures and on certain forms assumed by a group of particles upon vibrating elastic surfaces, Philos. Trans. R. Soc. London **121**, 299 (1831); On the forms and states of fluids on vibrating elastic surfaces, **52**, 319 (1831).
[10] J. Miles and D. Henderson, Parametrically forced surface waves, Annu. Rev. Fluid Mech. **22**, 143 (1990).
[11] M. Kharbedia, N. Caselli, D. Herráez-Aguilar, H. López-Menéndez, E. Enciso, J. A. Santiago, and F. Monroy, Moulding hydrodynamic 2D-crystals upon parametric Faraday waves in shear-functionalized water surfaces, Nat. Commun. **12**, 1130 (2021).
[12] S. T. Milner, Square patterns and secondary instabilities in driven capillary waves, J. Fluid Mech. **225**, 81 (1991).
[13] W. Zhang and J. Viñals, Square patterns and quasi-patterns in weakly damped Faraday waves, Phys. Rev. E **53**, R4283(R) (1996).
[14] C. Wagner, H. W. Müller, and K. Knorr, Faraday waves on a viscoelastic liquid, Phys. Rev. Lett. **83**, 308 (1999).
[15] L. Domino, M. Tarpin, S. Patinet, and A. Eddi, Faraday wave lattice as an elastic metamaterial, Phys. Rev. E **93**, 050202(R) (2016).
[16] P. Chen and J. Viñals, Pattern selection in Faraday waves, Phys. Rev. Lett. **79**, 2670 (1997).
[17] N. Tarasov, A. Perego, D. Churkin, K. Staliunas, and S. K. Turitsyn, Mode-locking via dissipative Faraday instability, Nat. Commun. **7**, 12441 (2016).
[18] B. Christiansen, P. Alstrom, and M. T. Levinsen, Ordered capillary-wave states: Quasicrystals, hexagons, and radial waves, Phys. Rev. Lett. **68**, 2157 (1992).
[19] H. Alarcón, M. Herrera-Muñoz, N. Périnet, N. Mujica, P. Gutiérrez, and L. Gordillo, Faraday-wave contact-line shear gradient induces streaming and tracer self-organization: From vortical to hedgehoglike patterns, Phys. Rev. Lett. **125**, 254505 (2020).
[20] L. D. Landau and E. M. Lifshitz, Fluid Mechanics, *Course of Theoretical Physics* (Pergamon, London, 1959), Vol. 6, p. 118.
[21] R. M. May, Simple mathematical models with very complicated dynamics, Nature (London) **261**, 459 (1976).
[22] N. Francois, H. Xia, H. Punzmann, S. Ramsden, and M. Shats, Three-dimensional fluid motion in Faraday waves: Creation of vorticity and generation of two-dimensional turbulence, Phys. Rev. X **4**, 021021 (2014).
[23] P. Coullet, L. Gil, and J. Lega, Defect-mediated turbulence, Phys. Rev. Lett. **62**, 1619 (1989).
[24] P. Unbanhowar, F. Melo, and H. L. Swinney, Localized excitations in a vertically vibrated granular layer, Nature (London) **382**, 793 (1996).
[25] D. I. Goldman, M. D. Shattuck, S. J. Moon, J. B. Swift, and H. L. Swinney, Lattice dynamics and melting of a nonequilibrium pattern, Phys. Rev. Lett. **90**, 104302 (2003).
[26] L. A. Lugiato and R. Lefever, Spatial dissipative structures in passive optical systems, Phys. Rev. Lett. **58**, 2209 (1987).
[27] I. Shani, G. Cohen, and J. Fineberg, Localized instability on the route to disorder in Faraday waves, Phys. Rev. Lett. **104**, 184507 (2010).
[28] V. Frumkin and S. Gokhale, Coupled instabilities drive quasiperiodic order-disorder transitions in Faraday waves, Phys. Rev. E **108**, L012601 (2023).
[29] G. B. Whitham, *Linear and Nonlinear Waves*, Wiley Series in Pure and Applied Faraday Mathematics (Wiley, New York, 1999).
[30] L. D. Landau and E. M. Lifshitz, Theory of Elasticity, *Course of Theoretical Physics* (Pergamon, London, 1959), Vol. 7, p. 127.
[31] W. S. Edwards and S. Fauve, Patterns and quasi-patterns in the Faraday experiment, J. Fluid Mech. **278**, 123 (1994).
[32] See Supplemental Material at http://link.aps.org/supplemental/10.1103/PhysRevResearch.6.043142 for details on experimental setup and the HC-setting considered in this paper.
[33] B. A. Puthenveettil and E. J. Hopfinger, Evolution and breaking of parametrically forced capillary waves in a circular cylinder, J. Fluid Mech. **633**, 355 (2009).
[34] C. Battle, C. P. Broedersz, N. Fakhri, V. F. Geyer, J. Howard, C. F. Schmidt, and F. C. MacKintosh, Broken detailed balance at mesoscopic scales in active biological systems, Science **352**, 604 (2016).
[35] L. D. Landau, On the problem of turbulence, in *Collected Papers of L. D. Landau*, edited by D. Ter Haar (Pergamon, London, 1965); Dokl. Akad. Nauk USSR **44**, 311 (1944).
[36] J. Goldstone, A. Salam, and S. Weinberg, Broken symmetries, Phys. Rev. **127**, 965 (1962).
[37] M. Stone, Lifetime and decay of excited vacuum states, Phys. Rev. D **14**, 3568 (1976).
[38] A. M. Kolmogorov, The local structure of turbulence in an incompressible liquid for very large Reynolds numbers, Dokl. Akad. Nauk SSSR **30**, 299 (1941); The local structure of turbulence in incompressible viscous liquid for very large Reynolds numbers, Proc. R. Soc. London, Ser. A **434**, 9 (1991).
[39] V. E. Zakharov and N. N. Filonenko, Energy spectrum for stochastic oscillations of the surface of a liquid, Sov. Phys. Dokl. **170**, 1292 (1966); Weak turbulence of capillary waves, J. Appl. Mech. Tech. Phys. **8**, 37 (1967).
[40] V. E. Zakharov and N. N. Filonenko, Stability of periodic waves of finite amplitude on the surface of a deep fluid, J. Appl. Mech. Tech. Phys. **9**, 190 (1968).
[41] V. E. Zakharov and L. A. Ostrovsky, Modulation instability: The beginning, Phys. D (Amsterdam) **238**, 540 (2009).
[42] G. Vanderhaegen *et al.*, Extraordinary" modulation instability in optics and hydrodynamics, Proc. Natl. Acad. Sci. USA **118**, e2019348118 (2021).
[43] L. D. Landau, On the theory of phase transitions, Zh. Eksp. Teor. Fiz. **7**, 19 (1937).
[44] H. Watanabe and H. Murayama, Redundancies in Nambu-Goldstone bosons, Phys. Rev. Lett. **110**, 181601 (2013).